

Entanglement of Square Nets in Covalent Organic Frameworks

Fangying Jin,[†] Ha L. Nguyen,[†] Zhiye Zhong, Xing Han, Chenhui Zhu, Xiaokun Pei, Yanhang Ma, and Omar M. Yaghi*[‡]



Cite This: *J. Am. Chem. Soc.* 2022, 144, 1539–1544



Read Online

ACCESS |



Metrics & More



Article Recommendations



Supporting Information

ABSTRACT: Two entangled 2D square covalent organic frameworks (COFs) have been synthesized from 4,4',4'',4'''-(9,9'-spirobi[fluorene]-2,2',7,7'-tetrayl)-tetrabenzaldehyde (SFTB) and *p*-phenylenediamine (PPA) and benzidine (BZD) to form COF-38, [(SFTB)(PPA)₂]_{imine}, and its isorecticular form COF-39, [(SFTB)(BZD)₂]_{imine}. We also report the single-crystal electron diffraction structure of COF-39 and find that it is composed of mutually entangled 2D square nets (sq1). These COFs represent the first examples of entangled 2D COF structures, which, as we illustrate, were made possible by our strategy of using the distorted tetrahedral SFTB building unit. SFTB overcomes the propensity of 2D COFs to stack through π - π stacking and allows entanglements to form. This work significantly adds to the design principles of COFs.

Covalent organic frameworks (COFs) are a class of extended structures formed by linking organic building units through strong covalent bonds.^{1–9} 2D COFs are often constructed by the combination of planar linking units facilitated by π - π stacking.^{3,5,9} For 3D COFs, the vast majority use nonplanar units^{10–12} to produce mainly bor,¹³ ctn,¹³ dia,¹⁴ pts,¹⁵ lon,¹⁶ acs,¹⁷ bcu,¹⁸ stp,¹⁹ ljh,²⁰ and ceq²¹ topologies. Although entanglements are well known for 3D COFs,^{15–17,22,23} they remain unknown for 2D COFs. The persistence of this state of affairs is likely due to the fact that the formation of 2D COFs has relied entirely on choosing planar building blocks and deploying π - π stacking as a means of organizing and ultimately crystallizing the material.^{24–26} In this Communication, we show how a distorted tetrahedral building block could be used to prevent π - π stacking and to allow 2D COF entanglements to form and therefore to increase the dimensionality of COFs from 2D to 3D.

Our strategy is based on using (4,4',4'',4'''-(9,9'-spirobi[fluorene]-2,2',7,7'-tetrayl)-tetrabenzaldehyde (SFTB), Figure 1a) as a building unit. Although the central carbon atom is tetrahedral, the overall geometry of the unit is a distorted tetrahedron, as determined by the arrangement that the aldehyde functionalities make with respect to each other. This unit, when reticulated with linear linkers, was expected to form a square net (Figure 1b). We also recognized that the distorted tetrahedral units, SFTB, should minimize π - π interactions and therefore encourage the formation of square entanglements rather than the usual stacking of layers. We have successfully implemented this strategy by the condensation of SFTB and *p*-phenylenediamine (PPA) or benzidine (BZD) to make 3D COFs (COF-38, [(SFTB)(PPA)₂]_{imine} and COF-39, [(SFTB)(BZD)₂]_{imine}, respectively) composed of an entanglement of 2D nets (Figure 1c). We believe that our strategy widens the scope of possible COF structures, where COF-38 and COF-39 are the first examples of entangled 2D COFs of any topology. It is worth mentioning that exhaustive efforts were undertaken to grow large crystals for COF-38, but only submicrocrystals

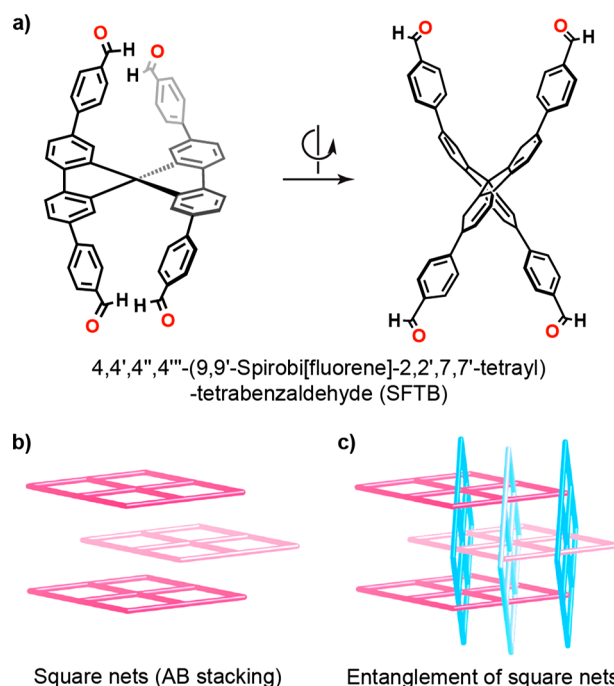
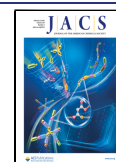


Figure 1. (a) Chemical structure of 4,4',4'',4'''-(9,9'-spirobi[fluorene]-2,2',7,7'-tetrayl)-tetrabenzaldehyde (SFTB). Illustration of (b) AB stacked square nets and (c) entanglement of square nets.

were obtained. However, we successfully synthesized a highly crystalline COF-39 sample for electron microscopy analysis

Received: December 22, 2021

Published: January 24, 2022



and elucidated its crystal structure. Therefore, we will discuss the synthesis and characterizations of COF-39 in the following content, whereas the synthesis and characterizations of isotreticular COF-38 are detailed in the Supporting Information (SI).

We synthesized SFTB using a slightly modified literature procedure and successfully crystallized this linker (SI, Section S2). We also determined the single-crystal X-ray structure of SFTB and found that it has a distorted tetrahedral geometry (SI, Section S3). The single-crystal structure of SFTB (Figure 2) clearly showed three independent as-symmetric units with

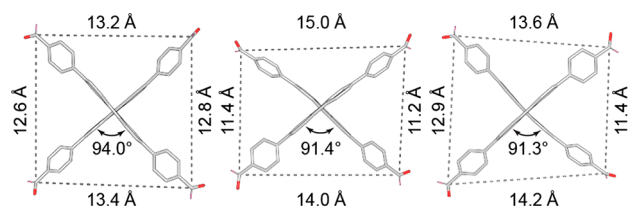


Figure 2. Single-crystal structure of SFTB showing three independent as-symmetric units with different edge lengths and dihedral angles.

different edge lengths measured counterclockwise from the aldehyde carbon to the adjacent carbon. The edge lengths were in the range between 11.2 and 15.0 Å. The average dihedral angle of two spirobi[fluorene] rings was 92.2°. The ratio of the rectangle sides in the SFTB linker was ~ 1.2 , indicating its distorted tetrahedral geometry. The rectangular rather than tetrahedral shape of SFTB played a role in producing the staggered COF framework and enhancing the flexibility of the extended structure (Figure 1b). SFTB was then reacted with linear amine-functionalized linkers PPA and BZD to form two 2D entangled COFs, namely, COF-38 and COF-39, respectively (Figure 3a).

COF-39 was synthesized solvothermally by reacting the linkers SFTB and BZD in a 1:2 molar ratio in trichlorobenzene with aqueous trifluoroacetic acid as a catalyst (SI, Section S2). The reaction mixture was sealed in a Pyrex tube and heated to 120 °C for 3 days. COF-39, a yellow precipitate formed at the bottom of the tube, was isolated by centrifugation and washed by Soxhlet extraction with anhydrous tetrahydrofuran for 18 h to remove unreacted reactants. The material was then solvent-exchanged with supercritical carbon dioxide and was finally activated under dynamic vacuum at room temperature for 1 h and then at 150 °C for 5 h. COF-39 was fully characterized by powder X-ray diffraction (PXRD), Fourier-transform infrared (FT-IR) spectroscopy, solid- and solution-state nuclear magnetic resonance (NMR) spectroscopies, elemental analysis (EA), thermogravimetric analysis (TGA), nitrogen sorption, scanning electron microscopy (SEM), and transmission electron microscopy (TEM) (SI, Sections S2–S9).

The FT-IR spectroscopy indicated the formation of imine linkages of COF-39 at $\nu_{\text{C=N}} = 1625 \text{ cm}^{-1}$ and the consumption of aldehyde starting material because there was no identifiable $\nu_{\text{C=O}}$ aldehyde stretching vibration at 1695 cm^{-1} remaining (SI, Section S4). Further confirmation of imine-linkage formation in COF-39 was shown by ^{13}C cross-polarization magic-angle spinning NMR spectroscopy (SI, Section S5), where the characteristic C=N imine resonances at 160 ppm were observed. Additionally, the disappearance of resonances above 190 ppm indicated that SFTB was fully converted into COF-39 by the imine condensation reaction.

The solution-state NMR analysis of acidic-digested COF-39 showed a stoichiometric ratio of 1:2 of SFTB/BZD, indicating that there were minimal defects in the COF-39 structure (SI, Section S5). The CHN analysis of COF-39 corresponded to a reticular formula of $[(\text{SFTB})(\text{BZD})_2]_{\text{imine}}$ (calcd for $\text{C}_{77}\text{H}_{48}\text{N}_4 \cdot 3\text{H}_2\text{O}$: C, 85.37; H, 5.02; N, 5.17%. Found: C, 85.94; H, 5.23; N, 5.29%; SI, Section S2) indicating that all water molecules were not fully removed in COF-39 (ca. 5.0%). These data agreed with the FT-IR spectroscopy and the TGA profile. The thermal stability of COF-39 was studied by TGA measured under a N_2 atmosphere, and the onset of the thermal decomposition of COF-39 was found to be at $\sim 480 \text{ }^\circ\text{C}$ (SI, Section S6).

The SEM micrographs of COF-39 showed a homogeneous morphology of $1 \mu\text{m}$ prism-shaped crystals (Figure 4a) formed by a conglomerate of thin and long needle-like crystals (SI, Section S7). The homogeneous morphology of COF-39 indicates phase purity, as also shown by TEM analysis (Figure 4b–e and SI, Section S8). Because of its high crystallinity, COF-39 exhibited a PXRD pattern with sharp peaks and low background (Figure 5). We were able to index at least 30 peaks from the PXRD pattern of COF-39 (SI, Section S8). The indexing result suggested that COF-39 crystallized in the tetragonal Bravais lattice with a space group of $I4_1$ or $I4$, which was in line with our hypothesis of having a 3D rather than a 2D COF structure.

For the TEM analysis (SI, Section S8), COF-39 was highly dispersed into ethanol, and several droplets of the suspension were subsequently dropped onto a carbon-coated copper grid for volatilization under ambient conditions. 3D electron diffraction (ED) data of COF-39 were collected to further elucidate the crystal structure.²⁷ A typical 3D ED data set with a resolution of $\sim 1.9 \text{ } \text{Å}$ is shown in the projections (Figure 4c). From the reconstructed 3D reciprocal lattice, a body-centered tetragonal Bravais lattice was identified (SI, Section S8), and the unit-cell parameters were determined to be $a = 39.9 \text{ } \text{Å}$, $c = 19.3 \text{ } \text{Å}$, and $V = 30\,654.6 \text{ } \text{Å}^3$.

On the basis of the information obtained from 3D ED, we tried to build the structural model of COF-39 in Materials Studio 8.0²⁸ using the tetragonal space groups $I4$, $\bar{I}4$, and $I4/m$. However, only the structural model built using $I4$ as the space group showed a chemically reasonable structure, and the simulated PXRD pattern showed great alignment with the experimental pattern (SI, Section S8). The unit-cell parameters were then refined by Pawley fitting against the experimental PXRD pattern: $a = 39.8 \text{ } \text{Å}$, $c = 19.2 \text{ } \text{Å}$, and $V = 30\,413 \text{ } \text{Å}^3$ with very low reliability factors ($R_p = 3.64\%$, $R_{wp} = 5.69\%$; Figure 5). More importantly, the calculated PXRD pattern of the built structure matched well with the experimental data of COF-39 (SI, Section S8).

According to the structural model, 2D sqI layers (Figure 3a) were formed by stitching together SFTB and BZD followed by the staggered stacking (AB-stacking form) of these formed layers along the c axis. The edge lengths of SFTB in COF-39 were found to be $8.4 \text{ } \text{Å} \times 16.4 \text{ } \text{Å}$. The rectangle side ratio was 2.0, larger than that of SFTB alone, indicating the high flexibility of the resulting framework. The dihedral angle of two spirobi[fluorene] rings in COF-39 was 92.5° (SI, Section S8). The wide opening of the rhombic windows within each of the layers and the high flexibility of building units triggered the entanglement of another identical net (Figure 3b). Accordingly, one set of staggered stacked layers entangled perpendicularly with another identical set to give rise to the

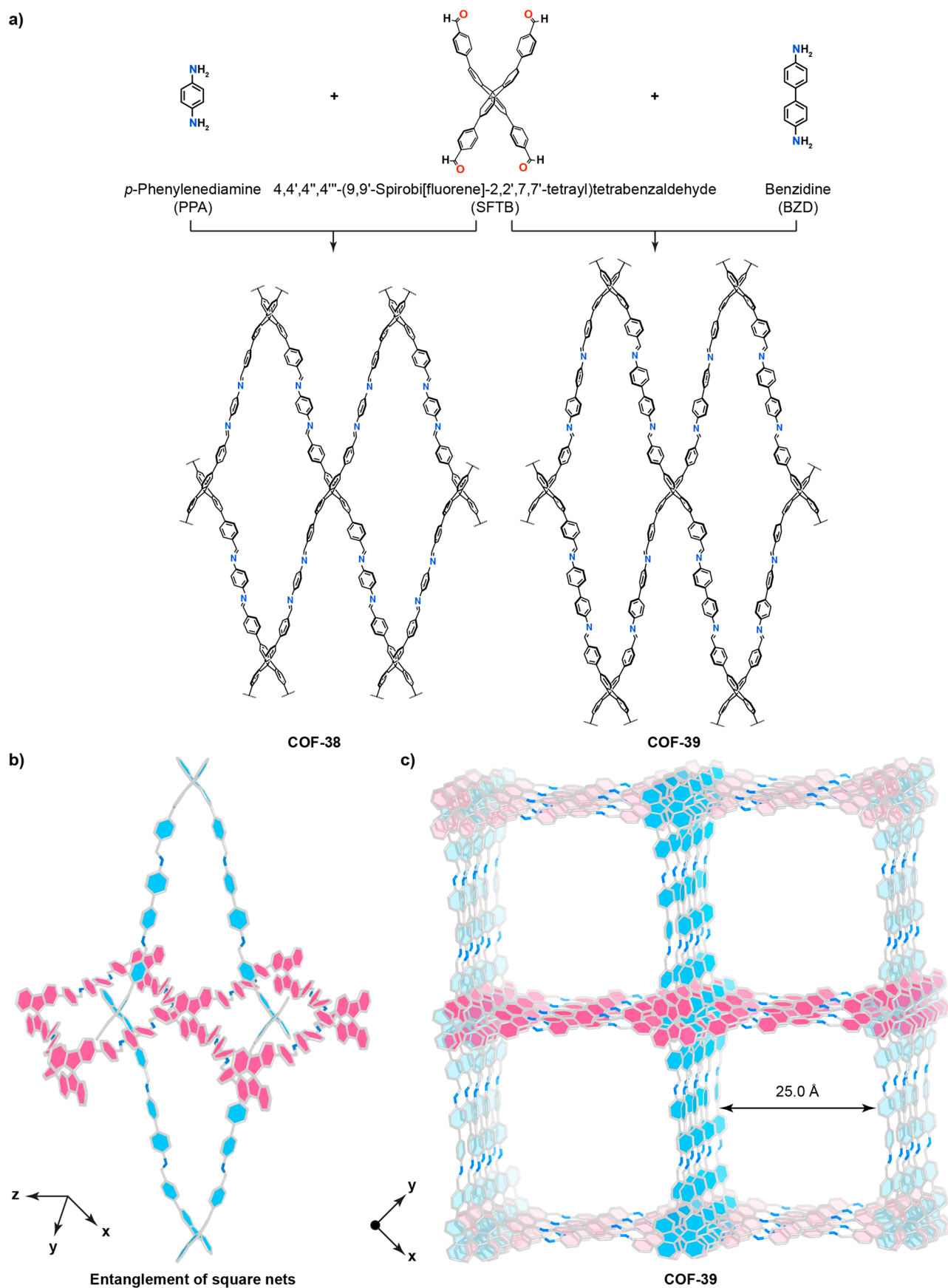


Figure 3. Strategy of constructing 3D COFs through the entanglement of squares. (a) 4,4',4'',4'''-(9,9'-Spirobi[fluorene]-2,2',7,7'-tetrayl)-tetrabenzaldehyde (SFTB) reacts with *p*-phenylenediamine (PPA) and benzidine (BZD) to form COF-38 and COF-39, respectively. (b) Entanglement of squares in COF-39. (c) Overall 3D structure shows 1D square channels in COF-39.

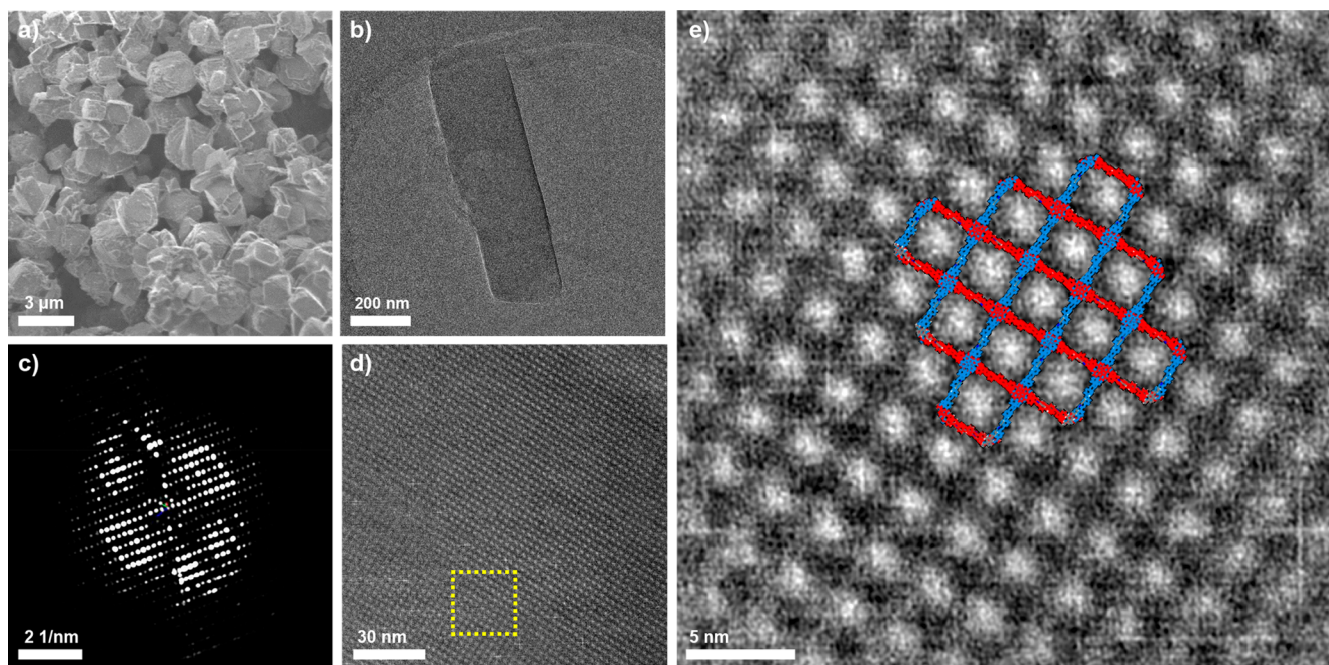


Figure 4. Electron microscopy data of COF-39. (a) Scanning electron microscopy (SEM) image of COF-39 presents a conglomerate of prismatic crystals. (b) Corresponding single crystal used for 3D ED data collection. (c) 2D projections of the 3D reciprocal lattice of COF-39 reconstructed from 3D ED data. (d) Average background subtraction filter (ABSF) high-resolution TEM (HRTEM) image of COF-39 taken along the [001] direction. (e) Magnified view of the highlighted area of panel d overlaid with a structure model showing good agreement along [001].

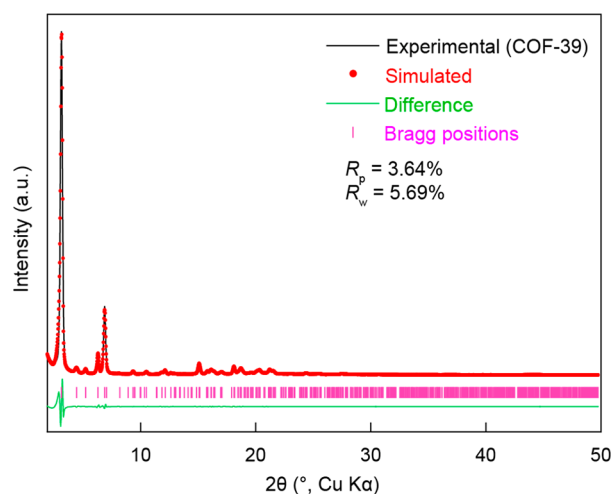


Figure 5. Pawley fitting (red circles) of experimental PXRD patterns (black lines) of an activated sample of COF-39.

final 3D framework adopting $sql-c^*$ as the topology with the 1D square channel along the [001] direction (Figure 3c).²⁹ From a topological perspective, COF-39 can also be classified based on the degree of catenation of 1/1 in a diagonal/diagonal fashion.³⁴ The crystal structure of COF-39 is completely different from that claimed to be a 3D COF with seven-fold *dia* topology reported by Liu and coworkers,³⁰ even though similar building units were used. It should be noted that the flexible and distorted tetrahedral units may act as an internal driving force to the entanglement formation. The detailed mechanism of the entanglement should be addressed in future studies.

High-resolution TEM (HRTEM) images were also taken to further gain insights into the crystal structure of COF-39. Indeed, the overlay of the structural model with the

experimentally obtained HRTEM images along both [001] and [111] showed good agreement (Figure 4e and SI, Section S8).

The permanent porosity of COF-39 was studied using N_2 sorption analysis at 77 K. Similar to entangled 3D COFs,^{16,19} COF-39 exhibited a Type I isotherm with a Brunauer–Emmett–Teller surface area of $813 \text{ m}^2 \text{ g}^{-1}$ (SI, Section S9). The Type I isotherm of COF-39 was likely attributed to the presence of water guest molecules, the structural flexibility, or the slight slipping of the layers from each other.

ASSOCIATED CONTENT

Supporting Information

The Supporting Information is available free of charge at <https://pubs.acs.org/doi/10.1021/jacs.1c13468>.

Synthesis and characterization details of COF-38 and COF-39 including elemental analysis, Fourier-transform infrared spectroscopy, nuclear magnetic resonance spectra, powder X-ray diffraction analysis data, electron microscopy data, computational modeling, N_2 sorption measurements, and thermogravimetric analysis (PDF)

Accession Codes

CCDC 2097659 and 2131421–2131422 contain the supplementary crystallographic data for this paper. These data can be obtained free of charge via www.ccdc.cam.ac.uk/data_request/cif, or by emailing data_request@ccdc.cam.ac.uk, or by contacting The Cambridge Crystallographic Data Centre, 12 Union Road, Cambridge CB2 1EZ, UK; fax: +44 1223 336033.

AUTHOR INFORMATION

Corresponding Author

Omar M. Yaghi – Department of Chemistry, University of California–Berkeley, Kavli Energy Nanoscience Institute at UC Berkeley, and Berkeley Global Science Institute, Berkeley,

California 94720, United States; Joint UAEU–UC Berkeley Laboratories for Materials Innovations, United Arab Emirates University, Al-Ain 15551, United Arab Emirates; orcid.org/0000-0002-5611-3325; Email: yaghi@berkeley.edu

Authors

Fangying Jin – Department of Chemistry, University of California–Berkeley, Kavli Energy Nanoscience Institute at UC Berkeley, and Berkeley Global Science Institute, Berkeley, California 94720, United States; orcid.org/0000-0002-0876-4473

Ha L. Nguyen – Department of Chemistry, University of California–Berkeley, Kavli Energy Nanoscience Institute at UC Berkeley, and Berkeley Global Science Institute, Berkeley, California 94720, United States; Joint UAEU–UC Berkeley Laboratories for Materials Innovations, United Arab Emirates University, Al-Ain 15551, United Arab Emirates; orcid.org/0000-0002-4977-925X

Zhiye Zhong – School of Physical Science and Technology, ShanghaiTech University, Shanghai 201210, China

Xing Han – Department of Chemistry, University of California–Berkeley, Kavli Energy Nanoscience Institute at UC Berkeley, and Berkeley Global Science Institute, Berkeley, California 94720, United States

Chenhui Zhu – Advanced Light Source, Lawrence Berkeley National Laboratory, Berkeley, California 94720, United States

Xiaokun Pei – Department of Chemistry, University of California–Berkeley, Kavli Energy Nanoscience Institute at UC Berkeley, and Berkeley Global Science Institute, Berkeley, California 94720, United States; orcid.org/0000-0002-6074-1463

Yanhong Ma – School of Physical Science and Technology, ShanghaiTech University, Shanghai 201210, China; orcid.org/0000-0003-4814-3740

Complete contact information is available at: <https://pubs.acs.org/10.1021/jacs.1c13468>

Author Contributions

[†]F.J. and H.L.N. contributed equally.

Notes

The authors declare no competing financial interest.

ACKNOWLEDGMENTS

We thank Dr. Cornelius Gropp (Yaghi Research Group) and Prof. George Lisensky (Beloit College) for valuable discussion. We thank Dr. Tianqiong Ma (Yaghi Research Group) for the SEM measurement of COF-38. We are grateful to Prof. Davide Proserpio (Università degli Studi di Milano) and Prof. Michael O’Keeffe (Arizona State University) for the helpful discussion on the nomenclature of the topology of COF-39. We acknowledge King Abdulaziz City for Science and Technology as part of a joint KACST–UC Berkeley collaboration and UAE University as part of a joint UAEU–UC Berkeley collaboration. We acknowledge the financial support from DOD Advanced Research Projects Agency award number HR00112020038. C.Z. acknowledges the financial support for the PXRD measurements at beamline 7.3.3 of the Advanced Light Source from DOE Office of Science User Facility under contract no. DE-AC02-05CH11231. Z.Z. and Y.M. acknowledge the financial support from the National

Natural Science Foundation of China (no. 21875140) and C \hbar EM SPST, ShanghaiTech University (no. EM02161943) for TEM measurements. We acknowledge the NIH (grant S10-RR027172) for financial support of the X-ray crystallographic facility at UC Berkeley and Dr. Nicholas Settineri for the support with using the facility. We acknowledge the College of Chemistry Nuclear Magnetic Resonance Facility for resource instruments, which are partially supported by NIH S10OD024998, and staff assistance from Dr. Hasan Celik and Dr. Alicia Lund.

REFERENCES

- (1) Yaghi, O. M.; Kalmutzki, M. J.; Diercks, C. S. *Introduction to Reticular Chemistry: Metal–Organic Frameworks and Covalent Organic Frameworks*; Wiley-VCH: Weinheim, Germany, 2019; pp 177–283.
- (2) Diercks, C. S.; Yaghi, O. M. The atom, the molecule, and the covalent organic framework. *Science* **2017**, *355*, 923.
- (3) Feng, X.; Ding, X.; Jiang, D. Covalent Organic Frameworks. *Chem. Soc. Rev.* **2012**, *41*, 6010–6022.
- (4) Kandambeth, S.; Dey, K.; Banerjee, R. Covalent Organic Frameworks: Chemistry beyond the Structure. *J. Am. Chem. Soc.* **2019**, *141*, 1807–1822.
- (5) Lohse, M. S.; Bein, T. Covalent Organic Frameworks: Structures, Synthesis, and Applications. *Adv. Funct. Mater.* **2018**, *28*, 1705553.
- (6) Haase, F.; Lotsch, B. V. Solving the COF trilemma: towards crystalline, stable and functional covalent organic frameworks. *Chem. Soc. Rev.* **2020**, *49*, 8469–8500.
- (7) Cote, A. P.; Benin, A. I.; Ockwig, N. W.; O’Keeffe, M.; Matzger, A. J.; Yaghi, O. M. Porous, Crystalline, Covalent Organic Frameworks. *Science* **2005**, *310*, 1166–1170.
- (8) Waller, P. J.; Gandara, F.; Yaghi, O. M. Chemistry of Covalent Organic Frameworks. *Acc. Chem. Res.* **2015**, *48*, 3053–3063.
- (9) Geng, K.; He, T.; Liu, R.; Dalapati, S.; Tan, K. T.; Li, Z.; Tao, S.; Gong, Y.; Jiang, Q.; Jiang, D. Covalent Organic Frameworks: Design, Synthesis, and Functions. *Chem. Rev.* **2020**, *120*, 8814–8933.
- (10) Guan, X.; Chen, F.; Fang, Q.; Qiu, S. Design and applications of three dimensional covalent organic frameworks. *Chem. Soc. Rev.* **2020**, *49*, 1357–1384.
- (11) Ma, X.; Scott, T. F. Approaches and Challenges in the Synthesis of Three-Dimensional Covalent–Organic Frameworks. *Commun. Chem.* **2018**, *1*, 98.
- (12) Nguyen, H. L. Reticular design and crystal structure determination of covalent organic frameworks. *Chem. Sci.* **2021**, *12*, 8632–8647.
- (13) El-kaderi, H. M.; Hunt, J. R.; Mendoza-cortes, J. L.; Cote, A. P.; Taylor, R. E.; O’Keeffe, M.; Yaghi, O. M. Designed Synthesis of 3D Covalent Organic Frameworks. *Science* **2007**, *316*, 268–272.
- (14) Liu, Y.; Ma, Y.; Zhao, Y.; Sun, X.; Gandara, F.; Furukawa, H.; Liu, Z.; Zhu, H.; Zhu, C.; Suenaga, K.; Oleynikov, P.; Alshammari, A. S.; Zhang, X.; Terasaki, O.; Yaghi, O. M. Weaving of Organic Threads into a Crystalline Covalent Organic Framework. *Science* **2016**, *351*, 365–369.
- (15) Lin, G.; Ding, H.; Yuan, D.; Wang, B.; Wang, C. A Pyrene-Based, Fluorescent Three-Dimensional Covalent Organic Framework. *J. Am. Chem. Soc.* **2016**, *138*, 3302–3305.
- (16) Ma, T.; Kapustin, E. A.; Yin, S. X.; Liang, L.; Zhou, Z.; Niu, J.; Li, L.; Wang, Y.; Su, J.; Li, J.; Wang, X.; Wang, W.; Sun, J.; Yaghi, O. M. Single-crystal x-ray diffraction structures of covalent organic frameworks. *Science* **2018**, *361*, 48–52.
- (17) Zhu, Q.; Wang, X.; Clowes, R.; Cui, P.; Chen, L.; Little, M. A.; Cooper, A. I. 3D Cage COFs: A Dynamic Three dimensional covalent organic framework with high-connectivity organic cage nodes. *J. Am. Chem. Soc.* **2020**, *142*, 16842–16848.
- (18) Gropp, C.; Ma, T.; Hanikel, N.; Yaghi, O. M. Design of higher valency in covalent organic frameworks. *Science* **2020**, *370*, No. eabd6406.
- (19) Li, H.; Ding, J.; Guan, X.; Chen, F.; Li, C.; Zhu, L.; Xue, M.; Yuan, D.; Valtchev, V.; Yan, Y.; Qiu, S.; Fang, Q. Three-Dimensional

Large-Pore Covalent Organic Framework with stp Topology. *J. Am. Chem. Soc.* **2020**, *142*, 13334–13338.

(20) Xie, Y.; Li, J.; Lin, C.; Gui, B.; Ji, C.; Yuan, D.; Sun, J.; Wang, C. Tuning the Topology of Three-Dimensional Covalent Organic Frameworks via Steric Control: From pts to Unprecedented ljh. *J. Am. Chem. Soc.* **2021**, *143*, 7279–7284.

(21) Li, Z.; Sheng, L.; Wang, H.; Wang, X.; Li, M.; Xu, Y.; Cui, H.; Zhang, H.; Liang, H.; Xu, H.; He, X. Three-Dimensional Covalent Organic Framework with ceq Topology. *J. Am. Chem. Soc.* **2021**, *143*, 92–96.

(22) Uribe-Romo, F. J.; Hunt, J. R.; Furukawa, H.; Klock, C.; O’Keeffe, M.; Yaghi, O. M. A Crystalline Imine-Linked 3-D Porous Covalent Organic Framework. *J. Am. Chem. Soc.* **2009**, *131*, 4570–4571.

(23) Ma, T.; Li, J.; Niu, J.; Zhang, L.; Etman, A. S.; Lin, C.; Shi, D.; Chen, P.; Li, L.; Du, X.; Sun, J.; Wang, W. *J. Am. Chem. Soc.* **2018**, *140*, 6763–6766.

(24) Alexandrov, E. V.; Blatov, V. A.; Proserpio, D. M. How 2-periodic coordination networks are interweaved: entanglement isomerism and polymorphism. *CrystEngComm* **2017**, *19*, 1993–2006.

(25) Haase, F.; Gottschling, K.; Stegbauer, L.; Germann, L. S.; Gutzler, R.; Duppel, V.; Vyas, V. S.; Kern, K.; Dinnebier, R. E.; Lotsch, B. V. Tuning the stacking behaviour of a 2D covalent organic framework through non-covalent interactions. *Mater. Chem. Front.* **2017**, *1*, 1354–1361.

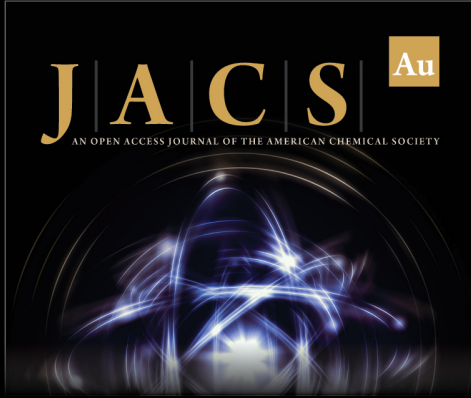
(26) Batten, S. R.; Robson, R. Interpenetrating Nets: Ordered, Periodic Entanglement. *Angew. Chem., Int. Ed.* **1998**, *37*, 1460–1494.

(27) Gemmi, M.; Oleynikov, P. Scanning Reciprocal Space for Solving Unknown Structures: Energy Filtered Diffraction Tomography and Rotation Diffraction Tomography Methods. *Z. Kristallogr. Cryst. Mater.* **2013**, *228*, 51–58.

(28) Dassault Systemes BIOVIA. *Materials Studio 8.0*; Dassault Systemes: San Diego, 2014.


(29) Bonneau, C.; O’Keeffe, M. High-symmetry embeddings of interpenetrating periodic nets. Essential rings and patterns of catenation. *Acta Crystallogr.* **2015**, *A71*, 82–91.


(30) Liu, Y.; Li, X.; Wang, S.; Cheng, T.; Yang, H.; Liu, C.; Gong, Y.; Lai, W.; Huang, W. Self-templated synthesis of uniform hollow spheres based on highly conjugated three-dimensional covalent organic frameworks. *Nat. Commun.* **2020**, *11*, 5561.



JACS Au
AN OPEN ACCESS JOURNAL OF THE AMERICAN CHEMICAL SOCIETY

Editor-in-Chief
Prof. Christopher W. Jones
Georgia Institute of Technology, USA

Open for Submissions 

pubs.acs.org/jacsau  ACS Publications
Most Trusted. Most Cited. Most Read.